J. theor. Biol. (2000) **203,** 285–301
doi:10.1006/jtbi.2000.1076, available online at http://www.idealibrary.com on IDEAL®

Modeling Plasma Virus Concentration during Primary HIV Infection

MAX A. STAFFORD*†‡, LAWRENCE COREY§, YUNZHEN CAO¶, ERIC S. DAAR||, DAVID D. HO¶, AND ALAN S. PERELSON**

*Computing and Mathematical Sciences Department, Texas A & M University-Corpus Christi, 6300 Ocean Drive, Corpus Christi, TX 78412, U.S.A., †Santa Fe Institute, 1399 Hyde Park Rd., Santa Fe, NM 87501, U.S.A., §Hutchison Cancer Research Center, Program in Infectious Disease, 1100 Fairview Avenue North, Seattle, WA 98109, U.S.A., ¶Aaron Diamond AIDS Research Center, The Rockefeller University, 455 First Avenue, New York, NY 10016, U.S.A., ||Cedars-Sinai Medical Center, Division of Infectious Diseases, Los Angeles, CA 90048, U.S.A. and **Theoretical Biology and Biophysics, Theoretical Division, Los Alamos National Laboratory, Los Alamos, NM 87545, U.S.A.

(*Received on* 9 *March* 1999; *Accepted in revised form on* 28 *December* 1999)

During primary HIV infection the viral load in plasma increases, reaches a peak, and then declines. Phillips has suggested that the decline is due to a limitation in the number of cells susceptible to HIV infection, while other authors have suggested that the decline in viremia is due to an immune response. Here we address this issue by developing models of primary HIV-1 infection, and by comparing predictions from these models with data from ten anti-retroviral, drug-naive, infected patients. Applying nonlinear least-squares estimation, we find that relatively small variations in parameters are capable of mimicking the highly diverse patterns found in patient viral load data. This approach yields an estimate of 2.5 days for the average lifespan of productively infected cells during primary infection, a value that is consistent with results obtained by drug perturbation experiments. We find that the data from all ten patients are consistent with a target-cell-limited model from the time of initial infection until shortly after the peak in viremia. However, the kinetics of the subsequent fall and recovery in virus concentration in some patients are not consistent with the predictions of the target-cell-limited model. We illustrate that two possible immune response mechanisms, cytotoxic T lymphocyte destruction of infected target cells and cytokine suppression of viral replication, could account for declines in viral load data not predicted by the original target-cell-limited model. We conclude that some additional process, perhaps mediated by CD8+ T cells, is important in at least some patients.

1. Introduction

During primary HIV infection, viral load increases sharply during the first few weeks after infection and then declines rapidly, ultimately reaching a quasi-steady state or set point level (Daar *et al.*, 1991; Schacker *et al.*, 1996; Kahn & Walker, 1998; Kaufmann *et al.*, 1998). Phillips (1996) suggested that the sharp decline in virus concentration might be the result of target-cell limitation, i.e., the running out of new cells for the virus to infect. Phillips demonstrated that simulations of a simple model based on this assumption produce a "spike" in virus concentration

‡Author to whom correspondence should be addressed.

0022–5193/00/070285 + 17 $35.00/0

qualitatively similar to that observed in patients. Another explanation for the viral decline is that an anti-viral immune response, for example, the cytotoxic T cell response (Koup *et al.*, 1994; Rinaldo *et al.*, 1995; Riviere *et al.*, 1995; Pantaleo *et al.*, 1997; Matano *et al.*, 1998; Schmitz *et al.*, 1999), brings the viral load in check. The question of whether the drop in viral load is primarily the result of an anti-viral immune response or target-cell limitation has yet to be answered satisfactorily.

This issue is addressed here by developing dynamic models of the events that occur during the first 100 days following primary HIV-1 infection, and comparing model predictions with clinical data. Models of primary infection have also been developed by Phillips (1996), Nowak *et al.* (1997a) and Murray *et al.* (1998). In addition, numerous models have been proposed to capture many of the features of progression to AIDS following the initial viral spike (Reibnegger *et al.*, 1989; Hraba *et al.*, 1990; Nowak *et al.*, 1990; McLean & Kirkwood, 1990; Nowak *et al.*, 1991; McLean & Nowak, 1992, Perelson *et al.*, 1993; Essunger & Perelson, 1994; Schenzle *et al.*, 1994; Stilianakis *et al.*, 1997; Kirschner *et al.*, 1998). A comprehensive model—one capable of predicting the spike, the asymptomatic phase, and progression to AIDS—is ultimately desired, but much can be learned by studying the early events. The characteristic spike in viral load provides a distinctive landmark against which differential equation models can be validated.

Figure 1 depicts the virus concentration in a representative HIV-positive patient studied at the Aaron Diamond AIDS Research Center. A viral spike similar to the one shown in Fig. 1 occurs in all ten patient data sets investigated. Our goal is to account for the initial rise, subsequent fall and stabilization of the virus concentration at a set-point level. To accomplish this, nonlinear least-squares estimation is applied to a simple target-cell-limited model of HIV-1 infection to determine parameters associated with each of the ten patient viral load data sets. We find that modest variations in the parameters of the model are capable of mimicking the wide patient-to-patient variation in the rise and initial decline in viremia. Following the initial decline, however, we find that the viral load in many patients falls below the quasi-steady-state viral load predicted by this model. We document this pattern, then explore two widely discussed methods of immune control that could account for the discrepancies—increased rate of killing of productively infected cells by cytotoxic T lymphocytes (CTLs) and suppression of viral production by CD8+ T cell antiviral factors (CAFs).

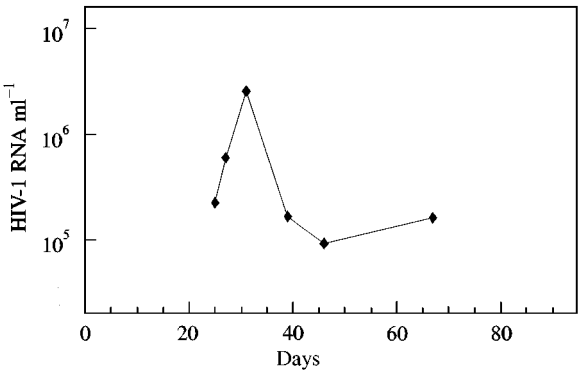

FIG. 1. Representative virus concentration time history. The time of initial infection is unknown so the point labeled $t = 0$ is arbitrary.

2. Parameter estimation

2.1. PATIENT DATA

Virus concentration measurements in peripheral blood from ten patients (Table 1) were obtained from three labs and used in parameter estimation. Data for patients 1 and 2 were from a University of Washington study (Schacker *et al.*, 1996), data for patients 3–9 were provided by the Aaron Diamond AIDS Research Center, and patient 10 data were provided by the Cedars-Sinai Medical Center in Los Angeles, CA.

Specimens were taken only after patients presented with acute infection symptoms, so baseline values of viral load are not available. The times in Table 1 for patient 1 are estimates of days since initial infection based on an average between the time of a recent HIV-negative sample and the first HIV+ sample. For patients 2 and 10 the times are measured from onset of symptoms, while for patients 3–9 they are taken from first date of data collection. Except for one patient, the time between initial infection and the time of the first data point is unknown and must be estimated. We discuss below how we estimated

TABLE 1
Virus concentration data

pt 1	pt 2	pt 3	pt 4	pt 5	pt 6	pt 7	pt 8	pt 9	pt 10
22, 27.2	3, 469.8	0, 766.8	0, 153.0	0, 228.2	0, 939.26	0, 1350.6	0, 2217.7	0, 216.4	4, 8057.2
43, 210	11, 1600	7, 947.6	5, 284.0	2, 599.2	3, 1485.0	4, 2398.6	4, 2427.9	5, 355.2	9, 9622.8
78, 85.9	15, 42.8	9, 706.2	6, 216.0	6, 2617.4	8, 701.6	9, 337.2	7, 2200.4	8, 355.4	10, 7830.0
106, 81.1	43, 41.7	15, 14.4	14, 143.0	14, 169.6	10, 564.0	12, 340.6	11, 1134.3	12, 146.8	14, 715.81
—	—	29, 2.3	21, 30.2	21, 93.7	15, 106.5	16, 202.3	14, 705.9	19, 100.9	16, 213.79
146, 46.2	71, 12.22	36, 1.1	32, 6.4	42, 165.6	17, 11.2	19, 169.7	18, 447.8	29, 34.7	18, 121.03
183, 60.1	99, 14.17	50, 1.0	39, 4.1	—	22, 87.3	23, 141.4	21, 412.7	57, 11.4	28, 16.36
230, 82.8	129, 18.2	57, 1.8	46, 5.85	98, 127.0	24, 20.6	26, 56.48	26, 302.1	—	30, 11.79
268, 103.	197, 70.8	64, 2.1		203, 65.9	29, 14.78	30, 182.75	29, 118.8	121, 17.3	35, 31.75
358, 72.1	255, 16.3			329, 144.7	36, 27.5	50, 267.0	33, 248.8	197, 90.1	42, 24.05
435, 79.4	330, 81.2				—	60, 182.7	36, 173.6	280, 68.2	51, 16.257
489, 70.4					64, 6.32	—	40, 131.3	376, 55.3	—
519, 207.					273, 2.27	213, 186.3	49, 259.1	525, 94.5	84, 19.59
534, 42.6					288, 5.64	551, 89.4	—	604, 34.4	177, 41.17
584, 10.8					347, 14.55		56, 132.24	645, 61.7	211, 61.95
610, 54.2					430, 13.6		63, 103.2	757, 55.9	239, 137.77
687, 22.3					478, 13.1		75, 117.1	776, 52.7	
778, 40.8							547, 5.62		
							659, 24.24		

Note: Data points are presented as ordered pairs with first number in each entry representing a relative time in days and the second number in each entry the virus concentration in thousands of HIV-1 RNA copies ml^{-1}. A horizontal line in a column indicates only the data points above the line were used in parameter estimation. All points were used if there is no horizontal line. The times listed for patient 9 are from 35 days following initial infection (Borrow *et al*., 1997). Patients (pt) 1 and 2 are patient numbers 1019 and 1113 from University of Washington study. Patients 3–9 are JSW-DAAR, CMO-DAAR, HOBR-SHAW, SUMA-SHAW, BORI-SHAW, INME-SHAW, and WEAU-SHAW from Aaron Diamond AIDS Research Center, respectively. Data for patient 10 are from patient DR from the Cedars-Sinai Medical Center in Los Angeles, CA.

the time shift, then use the time-translated data in subsequent graphs and discussions. Thus, for each patient the data in Table 1 will be translated forward in time by an amount τ.

The exact date of initial HIV-1 infection is known for patient 9 (Borrow *et al*., 1997; Clark *et al*., 1991). Values of time reported by Borrow *et al*., begin 15 days following onset of symptoms, which according to the patient, and corroborated by his sexual partner, was 20 days following initial exposure. Consequently, the data in Table 1 for patient 9, when translated forward 35 days reflect the actual rather than the estimated time following initial infection.

2.2. NONLINEAR LEAST-SQUARES PARAMETER ESTIMATION

We fit the data using a system of equations that include activated CD4+ T cells (T), productively infected CD4+ T cells (T^*), and virus concentration (V):

$$\frac{dT(t)}{dt} = \lambda - dT - kTV, \quad T(0) = T_0,$$

$$\frac{dT^*(t)}{dt} = kTV - \delta T^*, \quad T^*(0) = T_0^*, \qquad (1)$$

$$\frac{dV(t)}{dt} = \pi T^* - cV, \quad V(0) = V_0.$$

This form of the target-cell-limited model has been used in other studies (Nowak & Bangham, 1996; Nowak *et al*., 1997a; Bonhoeffer *et al*., 1997) and represents a minimal extension of models used to analyse drug perturbation experiments (Ho *et al*., 1995; Wei *et al*., 1995; Perelson *et al*., 1996; Perelson & Nelson, 1999), which have typically included only productively infected cells and virus concentration. The model lacks resting uninfected cells and latently infected cells, which have been included in other target-cell limited models (Perelson, 1989; McLean *et al*., 1991;

Essunger *et al.*, 1994; Phillips, 1996; DeBoer & Perelson, 1998). We ran numerous simulations using such models, but found that predicted viral load dynamics over the first 500 days did not differ appreciably from results obtained using eqn (1).

Here we only consider the primary targets for productive infection, activated CD4+ T cells (Schnittman *et al.*, 1990). While all cells bearing the CD4 molecule, such as T cells, dendritic cells and macrophages, are susceptible to infection, it has recently been found that more than 90% of productively infected cells in lymph tissue during primary infection are CD4+ T cells (Haase, 1999; Zhang *et al.*, 1999). It is possible for HIV to enter a resting cell, however direct infection of resting cells has been reported to be very inefficient due either to lack of full reverse transcription of viral RNA (Zack *et al.*, 1992) or lack of integration of the reverse transcribed DNA into the host cell's DNA (Stevenson *et al.*, 1990). Surprisingly, Zhang *et al.* (1999) found that early infection is not only propagated in activated and proliferating T cells, but also in resting T cells. A slight modification of our model would allow infection of resting cells but here we report results based on infection of only activated CD4+ T cells.

Activated cells are generated by activation of resting cells. As an approximation, the rate of their generation is assumed to be constant, with λ cells being produced per unit volume per unit time. A net loss of activated cells proportional to their number density is assumed to occur with rate constant d and represents the difference between loss from cell death and gain due to cell division. We assume that activated cells become infected at a rate proportional to the product of activated cell density and virus concentration with rate constant k, and that productively infected cells die with rate δ per cell. Productively infected cells are assumed to produce virions at an average rate of π per cell and virus is cleared with rate constant c.

Assuming that target cells are proliferating cells, we fix the density of target cells before infection, T_0, at 1% of the CD4+ T cell density in peripheral blood. This value is based on studies using the nuclear antigen Ki-67 (Sachsenberg *et al.*, 1998) that found the percentage of proliferating CD4+ T cells in the peripheral blood of healthy controls to be $1.1 \pm 0.6\%$. We assume there are no infected cells initially, so T_0^* is set to 0. We take the initial viral load, V_0, to be 10^{-6} virions ml^{-1} to represent the presence of a small number of virions present following primary infection. The exact value for V_0 is not critical since numerically it was found that varying V_0 over two orders of magnitude resulted in nearly identical virus concentration graphs except for a difference of less than 6 days in the predicted time to the viral peak. Thus, V_0 and the estimated translation time of the data, τ, will play off against each other. Before infection, we assume proliferating CD4+ T cells are at equilibrium, i.e. $\lambda = dT_0$. Hence, we need not estimate λ separately. We also accept the estimate from earlier studies (Perelson *et al.*, 1996) of the clearance rate constant, $c = 3\ \mathrm{day}^{-1}$, although somewhat higher values may be more appropriate (Mittler *et al.*, 1999; Ramratnam *et al.*, 1999). We show in the Appendix A that the behavior of the model depends on certain parameter products and ratios. Thus, for example, choosing a higher value of c will cause us to estimate a higher value of π. In the parameter range of interest, the model's behavior is only sensitive to the value of π/c. Similarly, choosing a different initial level of activated cells, T_0, can be compensated for by changes in π.

With assumed values for T_0, T_0^*, V_0, and c, we now estimate the remaining five parameters, d, k, δ, π, and τ for individual patients by minimizing the objective function

$$J(\theta) = \frac{1}{n} \sum_{i=1}^{n} (\log V(t_i) - \log \hat{V}(t_i))^2, \qquad (2)$$

where n represents the number of data points selected to estimate the vector of parameters, $\theta = [d,\ k,\ \delta,\ \pi,\ \tau]^{\mathrm{T}}$, $V(t_i)$ represents the virus concentration at time t_i predicted from the solution of eqn (1), and $\hat{V}(t_i)$ represents the data value at time t_i with all times in the data set having been shifted by τ.

Differences in logarithms, as opposed to differences in actual values, are used in forming the objective function to accommodate the large differences between the peak values and quasi-steady-state values after the peak. This approach

minimizes the sums of the squared logarithms of ratios of data values to simulation values and, hence, weights ratios of small data values equally with those of large ones. Using actual values resulted in a good fit of the peak itself, but in some cases this approach gave unrealistic values for the parameters and poor agreement during the times following the peak.

In all but one case we do not know the true value of the time shift, τ, of the data sets. For most of our patients, the time shift between initial infection and the first data point given in Table 1 can be expressed as the sum of two terms, $\tau = \tau_S + \tau_C$, where τ_S represents the time from initial infection to the onset of symptoms and τ_C is the time between onset of symptoms and the collection of the first viral load data. This is not applicable for patient 1, however, whose times are direct estimates from the date of initial infection based on the average time between a recent HIV-1 negative sample and the first HIV-positive sample. Thus, for patient 1, $\tau = 0$. The times for patients 2 and 10 were reported from the onset of symptoms, so $\tau_C = 0$ in these two cases. The times for patients 3–9 are from the day of initial collection of HIV-1 RNA data, so the time shifts for these patients contain both components.

Estimates of τ_S for 12 patients were reported by Schacker *et al.* (1996) with a range from 5 to 30 days. In addition, a value of $\tau_S = 20$ days was reported for patient 9 (Borrow *et al.*, 1997). Using the 12 reported values in Schacker and the value of 20 days reported for patient 9, we find a mean of 13 days from initial infection to onset of symptoms. Included in these estimates is the variability inherent in the time from initial transmission to when infectious virus first encounters target cells and infection takes off. Stochastic models during this early phase have been investigated by Merrill (1989). Other sources of variability include the replication and clearance rates of the virus.

Several factors enter into the value of τ_C—severity of symptoms, the time required for the patient to obtain an appointment to be seen by a physician, and whether a blood sample was taken on the first or a follow-up visit. Often the time from onset of symptoms to first collection is only a few days—patient 2 and patient 10, for example, had their first collection 3 and 4 days, respectively, following onset of symptoms. Sometimes, however, there was a lengthy period between first symptoms and data collection, such as for patient 9 whose reported τ_C was 15 days (Borrow *et al.*, 1997). We take 7 days as a representative value for τ_C which, combined with the mean of 13 days for τ_S, yields a time shift of $\tau = 20$ days which we apply to all patient data sets with the following exceptions. No time shift is applied to patient 1 as the times already represent estimates from day of initial infection. The shift for patient 9 is known exactly, as discussed above, so we use a shift of $\tau = 35$ days. Patient 10 reported having exposure 7 days prior to the onset of symptoms and although transmission could have occurred in a previous encounter, the high peak in viral load for this patient would be consistent with a short time from transmission to onset of symptoms. Consequently, we set $\tau = 7$ days for patient 10.

We summarize the parameter estimates for d, k, δ, π, and J for all patients (Table 2), though our values are not unique in light of the dependencies discussed in Appendix A. Figure 2 compares the predictions of the simplified model [eqn (1)], using the best-fit parameter values given in Table 2, with the time-shifted data for each of the ten patients. The figure illustrates the good agreement of the theory to the data with these parameter choices.

Using the default of $\tau = 20$ days can introduce inaccuracies in the other parameter estimates. Since the major source of variability in estimating each patient's parameters is probably the time of initial infection, we assessed this effect by estimating parameters using $\tau = 10$ and 30 days. The estimates for d at $\tau = 10$ and 30 days were on average 40% lower and 52% higher, respectively, than the values for $\tau = 20$ days. Similarly, the estimates of k were 130% higher and 39% lower than the estimates at $\tau = 20$ days. The variations in δ were less—11% lower at $\tau = 10$ days and 30% higher at $\tau = 30$ days. The production rate coefficient, π, was the only parameter whose estimates were not consistent in the direction of deviation from the 20-day estimate. The estimates at 10 days ranged from 50% higher to 30% lower than the estimate at day 20, while 6 of 7 estimates at day 30 were higher. The highest estimate at day 30 for π was 60% above the day 20 estimate.

TABLE 2
Estimated parameter values for patients 1–10

Patient	d (day^{-1})	k (μl virion-day^{-1})$\times 10^{-3}$	δ (day^{-1})	π (virion day^{-1})	J
1	0.013	0.46	0.40	980	0.046
2	0.020	0.36	0.80	1800	0.087
3	0.0065	0.64	0.43	960	0.050
4	0.0046	4.80	0.18	98	0.017
5	0.017	0.63	0.39	870	0.017
6	0.012	0.75	0.39	790	0.088
7	0.017	0.80	0.31	730	0.019
8	0.0085	0.66	0.17	830	0.0098
9	0.006	2.50	0.13	110	0.0033
10	0.0043	0.19	0.46	7100	0.063
Median	0.01	0.65	0.39	850	0.032
Sample SD	0.0057	1.4	0.19	2000	0.032

Note: Due to dependencies among parameters in the model (discussed in Appendix A) and an inability to estimate the time shift precisely, we present these estimated values only to summarize our findings. All estimates were performed using the program Adapt II (D'Argenio & Schumitzky, 1997).

We display median values for parameter estimates since there appear to be some extreme values in this small data set. For example, patient 9 was a rapid progressor (Borrow *et al.*, 1997) and the associated parameter estimates may be atypical as this patient's k is nearly the highest and his δ is the lowest of all the patients. It is unclear whether there is biological significance to these extremes, but it would be interesting to compare with estimates from other rapid progressors. Patient 10 is also atypical in that the estimate for k is the lowest and π the highest over all patients. Since, as shown in Appendix A, there is a family of parameter estimates associated with π and the initial value of target cells, T_0, the very high value of π may be more a reflection of this patient having more target cells. For example, if T_0 were 70 cells μl^{-1} rather than 10 cells μl^{-1} as assumed, the estimate for the viral production rate π would be $7100/7 = 1014$ virions day^{-1}, a value much more in line with the other patient estimates. Similarly, as discussed in Appendix A, a higher viral production rate coefficient would be predicted by our method if the viral clearance rate constant, c, were lower in this patient than normal.

The predicted steady-state values of productively infected cells, T_{ss}^*, and viral load, V_{ss}, are given in the second and third columns of Table 3. Eigenvalues of the approximate linear system, linearized about the steady-state solution, were found to have negative real parts (results not shown) assuring locally an asymptotically stable fixed point. The basic reproductive ratio, R_0, which represents the average number of new infected cells resulting from a single infected cell before any depletion of target cells (Bonhoeffer *et al.*, 1997), is provided in column 4. Virus concentration is growing exponentially during the initial rise, and we have tabulated the associated doubling time, T_2, in the last column of Table 3. The formulas used to compute T_{ss}^*, V_{ss}, R_0, and T_2 are taken from Bonhoeffer *et al.* (1997):

$$T_{ss}^* = \frac{\lambda}{\delta} - \frac{dc}{k\pi}, \quad V_{ss} = \frac{\pi\lambda}{\delta c} - \frac{d}{k},$$

$$R_0 = \frac{k\pi\lambda}{cd\delta}, \quad T_2 = \frac{\ln 2}{\delta(R_0 - 1)}.$$

3. Immune responses

We shall show that when patient data are examined over periods longer than 100 days after infection, the target-cell-limited model fails to explain the data in many patients, with the viral load falling below the prediction. However, by including immune response mechanisms the data can be explained.

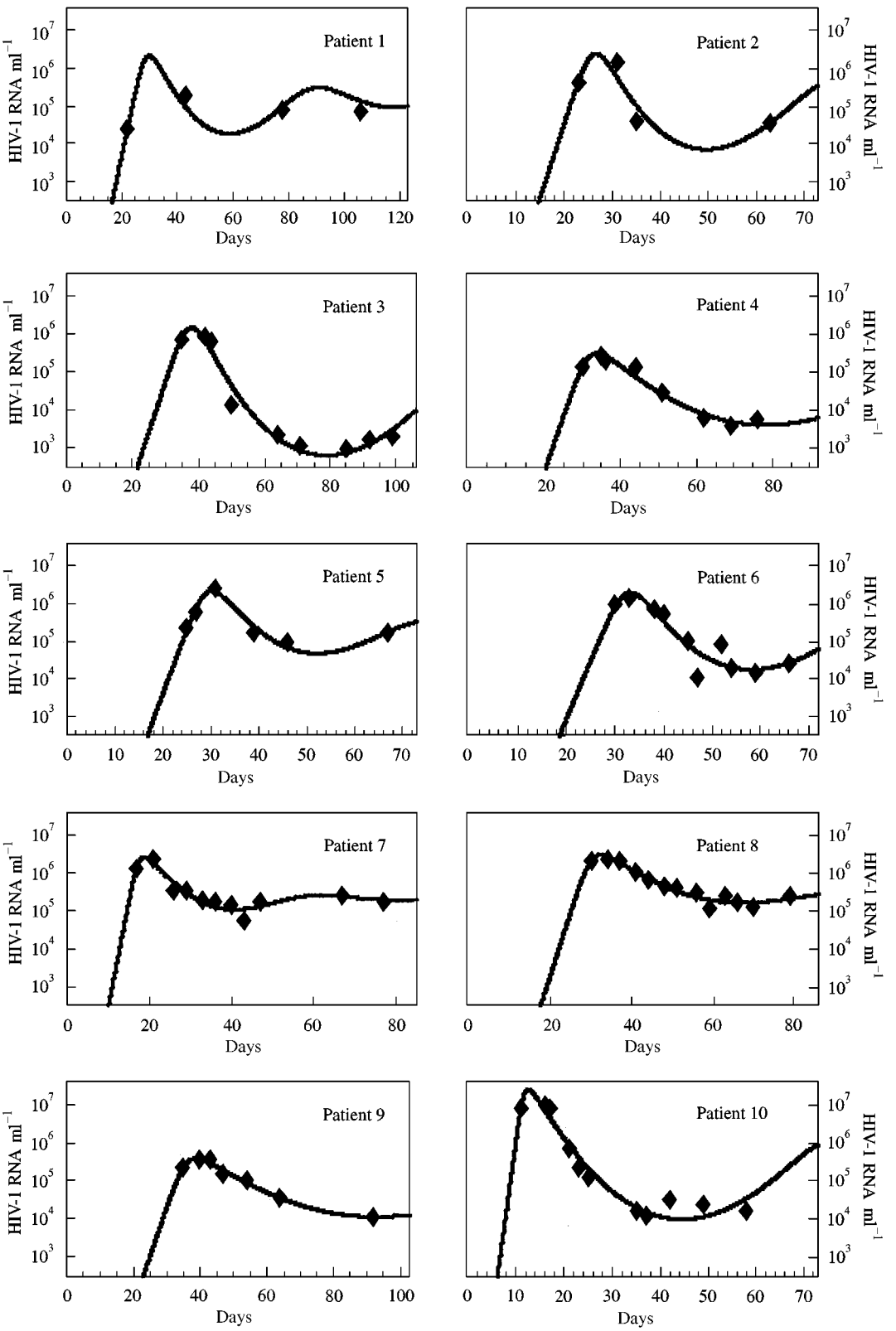

FIG. 2. Theoretical curves using estimated parameters vs. observed viral load data (◆) for all patients. Time values of the data points differ from those in Table 1 since all data sets have been translated in time as described in the text.

TABLE 3
Estimated steady state values of productively infected cell density (T_{ss}^*), viral load (V_{ss}), basic reproductive ratio (R_0), and doubling time (T_2)

Patient	T_{ss}^* (cells μl^{-1})	V_{ss} (RNA ml^{-1}) $\times 10^{-3}$	R_0	T_2 (days)
1	0.5	160	3.8	0.62
2	0.31	190	2.8	0.49
3	0.23	75	4.7	0.43
4	0.46	15	8.8	0.5
5	0.68	200	4.7	0.49
6	0.48	130	5.1	0.43
7	0.91	220	6.2	0.42
8	0.91	250	11.	0.42
9	0.77	27	6.6	0.94
10	0.17	400	9.6	0.17
Median	0.49	180	5.7	0.46
Sample SD	0.27	110	2.6	0.19

3.1. LONGER-TERM PREDICTIONS VS. DATA

Comparing the predicted behavior over longer intervals with the data (Fig. 3), we find that only some patients' viral loads are consistent with theoretical curves using short-term estimates of parameters. This appears to be the case for patients 1, 5 and 7. For example, patient 1's viral load following the peak declines at day 146 to a value that is approximately 30% of the steady-state value prediction based on only the first four data points, but there is a steady upward trend with the data point at day 268 reaching 65% of the predicted steady-state value. Patient 5's viral load drops only slightly below the predicted steady-state level (Fig. 3), then recovers. There are no data available for patient 7 between days 76 and 229, but we see that the predicted level is close to being attained by day 229.

Three patients were found to have statistically significant deviations from the model over longer time periods. Patients 2, 6 and 10 had objective function values more than five standard deviations higher than the short-term objective function mean over all ten patients. Patient 2's HIV-1 RNA concentration (Fig. 3) drops after the peak viremia to less than 10% of the steady-state value predicted using the first four data points and by one year is still approximately 40% of the predicted steady-state level. After the peak in viremia, the viral load of patient 6 falls well below the predicted steady-state level and remains below. Again, the model does not adequately explain viral load declines of this magnitude. Although patient data through day 100 were used for most patients, patient 8 data after day 69 were not used. The reason for this exclusion is that the minimum objective function value including these points was approximately double the minimum value excluding the points. In Fig. 3 we see the data points between days 76 and 95 fall below the theoretical curve in a pattern consistent with patients 2, 6 and 10. The viral load of patient 10 falls well below the predicted steady-state level, but during days 191–246 there is a steady-increase toward the steady-state value predicted by the model.

Patient 9 (Fig. 3) is an exception to the general trend. The final four points displayed were not used in the parameter estimation, and although the first point of these four agrees with the simulation, the final three are above the predicted steady-state value. This patient was atypical in that he progressed to AIDS in less than 3 years (Borrow *et al.*, 1997), and thus unlike slower progressors may not have had any protective immune response arise or, alternatively, may have had a particularly cytopathic strain of virus.

In cases where viral load declines substantially after the peak, as is the case for patients 3, 6 and 10 (Fig. 2), the simple target-cell-limited model predicts solutions that are highly oscillatory during their approach to the steady-state (Fig. 3). Minimum viral loads following the peak for these three patients are approximately 1000, 11 000 and 12 000 HIV-1 RNA copies ml^{-1}, respectively, compared with predicted steady-state values of 75 000, 130 000 and 400 000 HIV-1 RNA copies ml^{-1} (Table 2). Insufficient data exists in these three cases to verify or refute the model's predictions of the one to two order of magnitude increases from the minima to the steady-state levels, but such oscillatory behavior is not typically seen in data. Some additional HIV patient data (Fig. 4) show that viral load does not always rebound as the model would predict following steep declines. (Although there were no data points available to define the peak for these patients, parameter values similar to those in Table 2 were used to generate theoretical curves shown in Fig. 4.) The model's predictions clearly do not

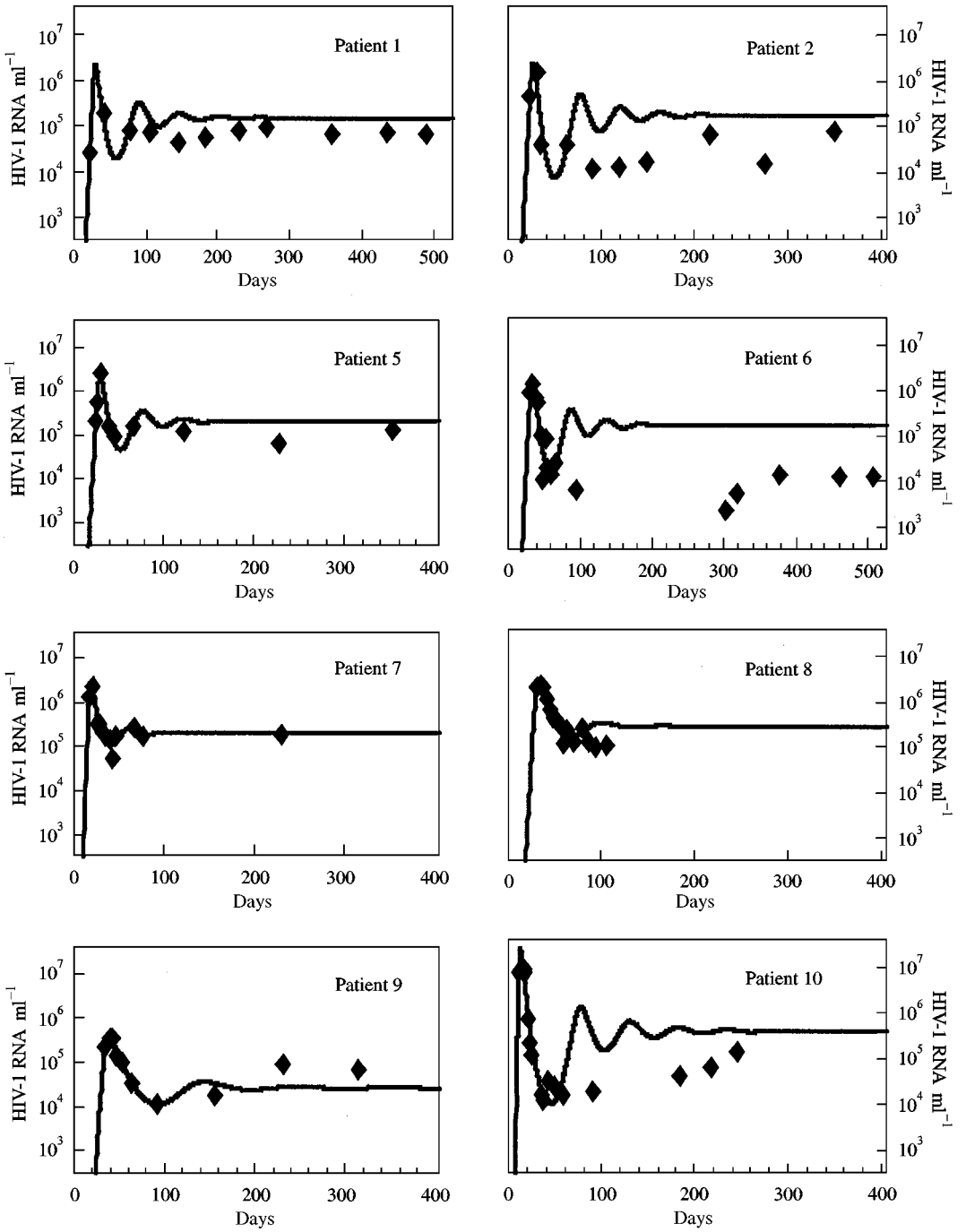

FIG. 3. Theoretical curves over longer intervals generated with best-fit parameters estimated using data only from the first 100 days. Long-term data for patients 3 and 4 were not available. In some cases (patients 1, 5, 7) the prediction from the first few points is consistent with data while in other cases (patients 2, 6, 10) the viral load is generally below the prediction. Patient 9 is atypical in that he rapidly progressed to AIDS (Borrow *et al.*, 1997).

agree with patient data in the region just beyond the local minima at days 35 and 70, respectively.

On the other hand, viral loads of patients 1, 2, 5, 7 and 10 do return approximately to the steady-state values predicted by the model (Fig. 3). Additionally, Nowak *et al.* (1997a) report two cases of SIV-infected macaques whose SIV RNA levels increase more than an order of magnitude

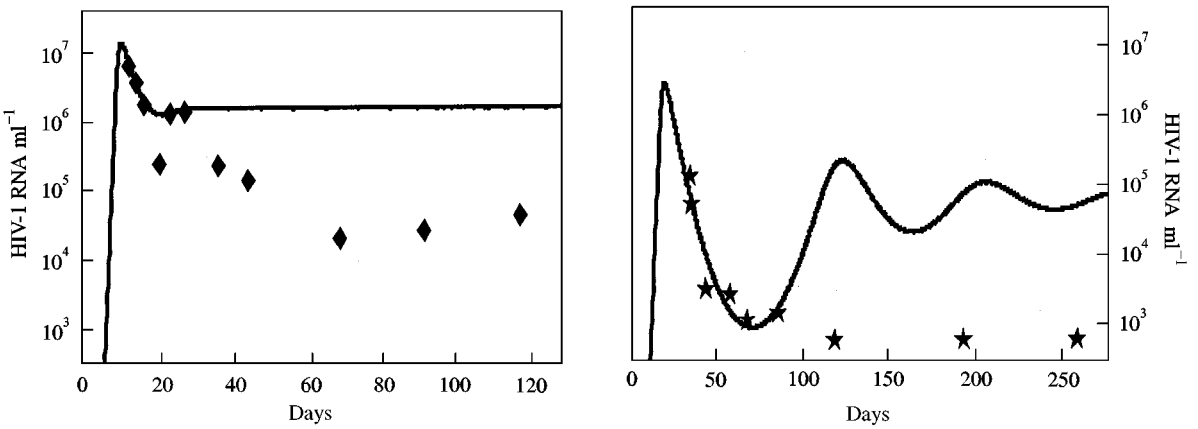

FIG. 4. Theoretical curves using estimated parameters compared with two additional data sets from Aaron Diamond AIDS Research Center: VS (◆) and MM (★). Although no data exist for these patients near the peak, approximate values to mimic the rise and decline until the first local minimum in each case were determined. The target-cell-limited model does not appear to be capable of matching these data sets.

between 35 and 119 days post-infection. Comparing this data with patient 3, the patient exhibiting the most pronounced decline, we note that the model predicts a rise of less than two orders of magnitude from the lowest HIV concentration value.

In summary, using longer-term data we find significant deviations in viral load in some patients from the target cell limited model's predicted values. Specifically, patients 2, 6 and 10 (Fig. 3) had significantly lower viral loads as early as 84 days following initial infection. Patients 1, 5 and 8 had viral loads slightly below the predicted values, and patient 7 showed no deviation from predicted viral load (although there were no data points between days 80 and 233). Only patient 9 had an increase above the predicted steady-state value, the increase occurring 242 days following initial infection. To explain the lower than predicted viral loads, we speculate that some patients produce an immune response capable of reducing viral burden. To explore this possibility, we modified our model to predict what might happen if there were either HIV-specific cytotoxic T lymphocyte (CTL) activity or suppression of HIV replication by cytokines such as IL-16 (Maciaszek *et al.*, 1997) or CAF (Mackewicz *et al.*, 1995).

3.2. MODELS OF TWO POSSIBLE IMMUNE RESPONSE MECHANISMS

Typically immune responses are strongest when antigen levels are high. Here, as a first examination of the potential effects of an immune response, rather than attempting to model the full CTL response we simply assume that δ, the death rate constant of productively infected cells, increases due to CTL-mediated cytolysis. The increase is assumed to be dependent upon the number of productively infected cells, which in turn is proportional to the virus concentration. Because the immune response takes time to develop, we assume that CTL activity is not substantial until after the peak viremia is reached. We make this assumption because several graphs of patient data seem to indicate that abrupt changes from the simple model's predictions occur most often as the viral load begins to climb for a second time. A similar delay has been reported in chimpanzee hepatitis B virus (HBV) infection (Guidotti *et al.*, 1999) where CD8+ T cells did not appear in significant numbers until 16 weeks after initial infection.

In our analysis, we use the parameter values estimated over the first 100 days with the exception that we now model CTL-induced changes in δ with viral load as follows:

$$\delta = \delta_0 + \delta_1(V) \quad \text{where } \delta_1(V) = \begin{cases} 0, & t < t_1, \\ f(t)V, & t \geq t_1, \end{cases}$$

The function $f(t)$ is chosen to increase with time over several days to mimic effector cell expansion beginning at $t = t_1$, and to decline gradually beginning at $t = t_2$ simulating subsequent loss of

effector cells. We selected the functional form

$$f(t) = \frac{\beta}{1 + \kappa e^{-(t-t_1)/\Delta T_1}} - \frac{\beta}{1 + \kappa e^{-(t-t_2)/\Delta T_2}},$$

but other forms would likely give similar results.

The simple model [eqn (1)] does not accurately predict the viral load after day 75 for patients 2, 6 and 10 (Fig. 3). Incorporating a CTL response as described above, we find (Fig. 5) that the model can now mimic patient 2 data between days 90 and 230. Using the same functional form for δ, we obtained similar results for patients 6 and 10 (Fig. 5). Patients 2 and 10 seem to lose the ability to contain the virus as their viral loads increase within a year of initial infection to nearly the steady-state values predicted by the target-cell-limited model. Patient 6, however, maintains a low quasi-steady-state.

We set $\kappa = 1 + 10^5\beta$, $\Delta T_1 = 2.5$ days and $\Delta T_2 = 15$ days for all simulations, and summarize in Table 4 the remainder of the parameter values used in the function $f(t)$. These parameter estimates are not claimed to be unique and we have not attempted to accurately determine their values, since the point of this work was simply to show that an immune control mechanism, such as cytotoxic T lymphocyte activity, could mimic the longer-term behavior in some patients. While the function $f(t)$ has sufficed for this purpose, further work will be needed to elucidate an appropriate quantitative description of the CTL response.

The time variations in δ, the death rate constant of productively infected cells, shown in Fig. 6, demonstrate that a transient increase and decline in the rate of killing of infected cells is needed to explain the data for patients 2 and 10, but a more permanent increase was needed to explain the data for patient 6. The magnitudes of the increases appear to require unrealistically high values for δ since estimates for this parameter typically range from around 0.2 day to 0.9 day^{-1} in drug perturbation experiments (Klenerman *et al.*, 1996; Wu *et al.*, 1999).

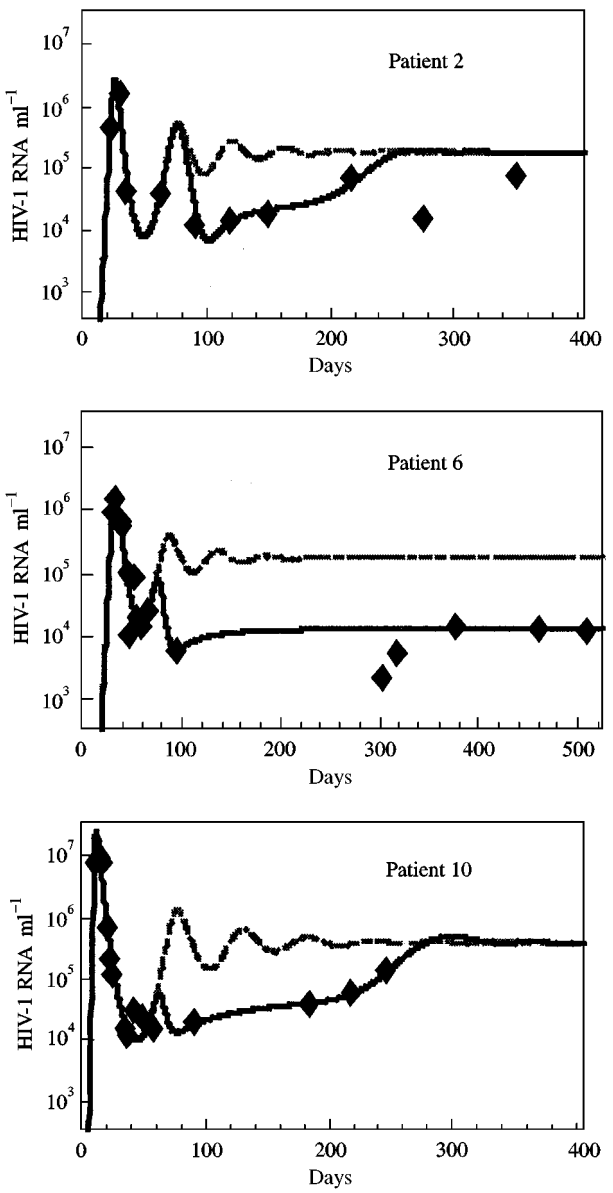

FIG. 5. Theoretical curves with simulated CTL response (solid curve), theoretical curve without simulated CTL response (dashed curve), and data points (◆) for patients 2, 6 and 10.

TABLE 4

Times of onset (t_1), decline (t_2) and relative strength (β) of the CTL response as defined by the function $f(t)$

Patient	t_1 (days)	t_2 (days)	β μl(virion-day)$^{-1}$
2	60	65	0.09
6	50	—*	0.125
10	45	100	0.070

*Patient 6 viral load was maintained well below the predicted steady-state value for more than 500 days, so no decline in CTL response with time was modeled.

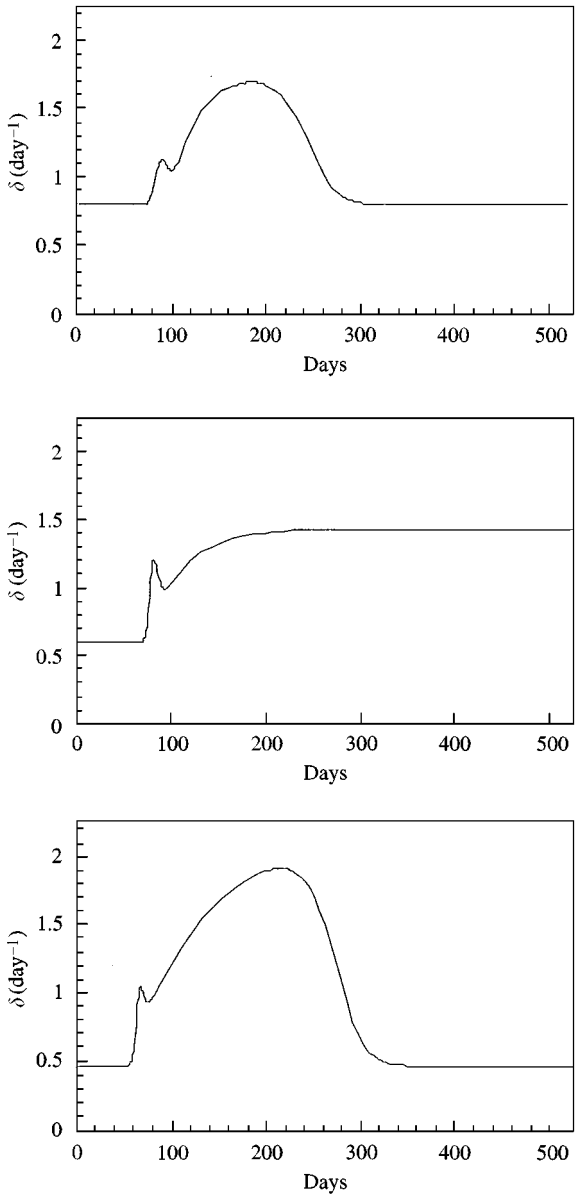

FIG. 6. Inclusion of a CTL response causes the infected cell death rate constant, δ, to change over time as shown above for patients 2, 6, and 10.

Another immune mechanism that has been suggested (Walker *et al.*, 1986; Mackewicz *et al.*, 1995; Jin *et al.*, 1999) is that a soluble factor produced by CD8+ T cells partially inhibits the production of virus particles by productively infected cells. The identity of this factor is unknown but Levy and co-workers have called it CAF, CD8+ T-cell antiviral factor (Mackewicz *et al.*, 1995). We crudely simulated this form of response by reducing the virus production rate coefficient, π, to 35% of its original value at

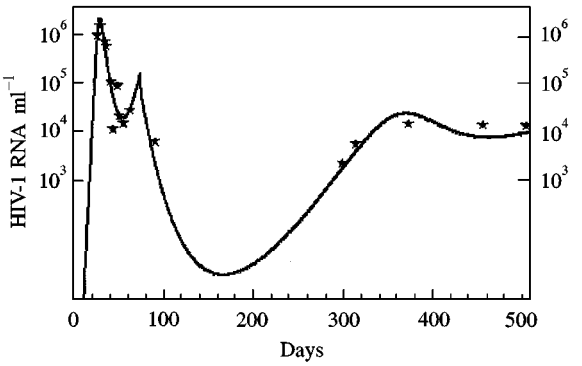

FIG. 7. Theoretical curve for patient 6 incorporating a crude model of cytokine-mediated viral suppression. The production rate coefficient, π, was reduced to 35% of its value at day 70. If the change in π were made gradually then the sharp peak at day 70 could be converted into a more gradual change.

a time shortly following the first minimum in viral load. This yielded results for patient 6 that are similar to the data (Fig. 7). Interestingly, Jin *et al.* (1999) found that increasing π about three-fold gave reasonable agreement with viral load increases observed in SIV-infected macaques after they were CD8+ T cell depleted.

4. Discussion

Although many complex processes occur during the rise and fall in viral load following initial HIV infection, we have shown that temporal changes in virus concentration observed early after infection are consistent with the assumptions embodied in the simple target-cell limited model [eqn (1)]. Relatively small variations in parameters determined by the host (d) and parameters determined by interaction between host and virus (k, δ, and π) can be used to account for the highly diverse patient-to-patient viral concentration transients observed during the first 100 days following primary infection.

We found a mean and median value of 0.37 and 0.39 day^{-1}, respectively, for δ over our ten patients. These values are slightly less than the population estimate of 0.47 day^{-1} obtained for the first phase decay rate constant obtained by Wu *et al.* (1999) in a drug perturbation study of 48 patients analysed using a nonlinear mixed-effect model. Our estimate is consistent with the mean value of 0.37 day^{-1} determined by

Klenerman *et al.* (1996) using data from five different drug perturbation experiments, and slightly lower than the first-phase decay rate constant of 0.5 day^{-1} obtained by Perelson *et al.* (1996). In a separate study, a mean of 0.38 day^{-1} for δ was observed in primary infection patients given combination therapy a few days following onset of symptoms (Little *et al.*, 1999).

We are unable to validate our results for the other parameter estimates as no conclusive, independent estimates, other than for δ, have been published to date. Further, dependencies between π and T_0 and between π and c, as shown in Appendix A, imply that our estimates of π, c and T_0 are not unique.

Our results support, but do not conclusively prove, that the initial decline in viral load is due to target-cell limitation, as suggested by Phillips (1996), rather than to a response by the immune system. The model, which can be viewed as a minimal extension of the two-equation model widely used to interpret drug perturbation experiments (Perelson *et al.*, 1996; Perelson & Nelson, 1999), is able to match the highly diverse initial viral load transients by minor modification of parameters.

Three arguments are often given to support the hypothesis of immune system control during primary infection. First, there is evidence of a temporal correlation between an increase in CTL precursor frequency and decline in viral load (Koup *et al.*, 1994). Second, an inverse correlation between the steady-state level of plasma virus and the number of effector CTLs has been observed (Ogg *et al.*, 1998). Third, Matano *et al.* (1998) used anti-human CD8+ monoclonal antibody to deplete CD8+ T cells in macaques, either a few days before or a few days after inoculation with simian immunodeficiency virus (SIV). Measurements of SIV concentration showed marked increases in peak viremia as compared to controls, suggesting that CD8+ T cells are responsible for controlling the viral load.

These studies do not provide direct evidence, however, that CTLs are causing the HIV-1 viral load to decline from its early peak level. It may well be that many cytotoxic cells are generated as viral load increases and then, as viral load declines, the antigenic stimulus diminishes and the CTLs also decline. Thus, the temporal correlation of CTL and virus as well as the inverse correlation between viral load and CTL do not establish to what extent CTLs are controlling the virus or simply responding to changes in antigen load. Further, *in vitro* it has been shown that the HIV-1 protein *nef* causes down regulation of MHC class I molecules on HIV-infected cells making such cells poor targets for cytolytic killing (Collins *et al.*, 1998). Thus, while CTLs have the potential to shorten the lives of productively infected cells, these cells may be poor targets and, due to viral cytopathic effects, may already have a short lifespan. Perhaps an even stronger argument is that CTL activity during primary infection varies widely among HIV-1 patients (Musey *et al.*, 1998), yet all ten of our patients' viral loads decline significantly from their peak values. Thus, it is not clear to what extent the large frequencies of CTLs observed in some studies are responsible for effectively eliminating productively infected cells, and hence causing the large drop in viral load observed during the first 30–50 days following initial infection.

The observation that anti-CD8 antibodies cause an increase in plasma virus levels supports the notion of CD8+ T cells playing a role in the control of viremia, although this effect may be mediated by soluble factors rather than CTL action. Also, the experiment by Matano *et al.* (1998) is not definitive, as there is a plausible alternative explanation of their observations. We note that administration of anti-CD8 antibody to control animals AH37 and T14 generates significant changes in CD4+ T cell levels as well as CD8+ T cell levels. In fact, these animals' CD4+ T cell levels decline to approximately 25 and 50% of their respective baseline values by 7 days following anti-CD8 monoclonal antibody injection. Such a significant change in the CD4+ T cell population implies that the monoclonal antibody does not simply remove CD8+ T cells. Major changes in cytokine production and in the degree of activation of CD4+ T cells may well be occurring, which in turn could significantly alter the virus concentration. The target-cell-limited model, in fact, predicts much higher peak levels in viremia if the number of activated cells present at the time of initial infection is increased. We speculate that the low levels of CD4+ T cells found in the

periphery 7 days after injection with anti-CD8 monoclonal antibody is the result of their activation and death or sequestration in lymph nodes. The anti-CD8 antibody might be inducing pro-inflammatory cytokines that simultaneously constrict the efferent lymph node ducts and produce an increase in activated CD4+ T cells that are SIV-susceptible.

In another SIV experiment (Schmitz *et al.*, 1999), additional evidence is presented that suggests CD8+ T cells control viral load immediately following the peak in some monkeys. Again, anti-CD8 monoclonal antibodies were used to deplete the CD8+ T cells. Here, viral loads were only reported from the peak onwards. Although all five control animals had approximately the same peak values in viral load as those whose CD8+ T cells had been depleted, those with depleted CD8+ T cells on average maintained higher viral loads in the 28 days following the peak. In this experiment, unlike results reported in Matano *et al.* (1998), the presence of CD8+ T cells did not affect the magnitude of the peak viral load since both the controls and the CD8-depleted animals had similar peak values.

In summary, although CD8+ T cells may influence viral load, the effect seen by Schmitz *et al.* (1999) occurred after the peak. Our models of primary infection also suggest that if CD8+ T cells are playing a role in primary infection, their main effect is seen predominantly late in the response and may not be directly responsible for bringing the peak viremia down. More detailed experimental studies coupled with models of CD8+ T cell activity, will be needed to more precisely elucidate the role of CD8+ T cells in primary infection.

5. Summary

We have shown that a frequently used target-cell-limited model can mimic the highly diverse temporal changes in viral load of ten patients during the first 100 days or so of primary HIV-1 infection. These results are consistent with, and provide evidence for, target cell limitation being the principle cause of the initial decline in viral load following the initial viremia peak.

The standard target-cell-limited model accurately predicts viral load in some patients well beyond the initial transient, but in other patients the viral load falls far below the model's prediction. This suggests that one or more unmodeled processes that lower the viral load are present in these patients. We have explored two such processes—cytotoxic T lymphocyte (CTL) destruction of productively infected cells and suppression by CD8+ T cell antiviral factor (CAF). We find that models that include either one of these effects can mimic patient data, but thus far we are unable to clearly identify one or the other as dominant. Partial evidence in favor of CAF over CTL was obtained, however, since unrealistically high values of the productively infected death rate constant were needed to match the data in the three patients we considered.

Portions of this research were done under the auspices of the U.S. Department of Energy. It was supported by faculty fellowships awarded to MAS by the Associated Western Universities and the American Society of Engineering Education, the Santa Fe Institute, the Jeanne M. Sullivan and Joseph P. Sullivan Foundation, NIH grants RR06555 and AI40387, and a research grant from Texas A & M University-Corpus Christi. We thank George Shaw, University of Alabama, for providing samples from his primary infection patients for analysis and the patients who participated in the clinical trials.

REFERENCES

BONHOEFFER, S., MAY, R. M., SHAW, G. M. & NOWAK, M. A. (1997). Virus dynamics and drug therapy. *Proc. Nat. Acad. Sci. U.S.A.* **94,** 6971–6976.

BORROW, P., LEWICKI, H., WEI, X., HORWITZ, M. S., PEFFER, N., MEYERS, H., NELSON, J. A., GAIRIN, J. E., HAHN, B. H., Oldstone, M. B. A. & Shaw, G. M. (1997). Antiviral pressure exerted by HIV-1-specific cytotoxic T lymphocytes (CTLs) during primary infection demonstrated by rapid selection of CTL escape virus. *Nat. Med.* **3,** 205–211.

CLARK, S. J., SAAG, M. S., DECKER, D. W., CAMPBELL-HILL, S., ROBERSON, J. L., VELDKAMP, P. J., KAPPES, J. C., HAHN, B. H. & SHAW, G. M. (1991). High titers of cytopathic virus in plasma of patients with symptomatic primary HIV-1 infection. *New Engl. J. Med.* **324,** 954–960.

COLLINS, K. L., CHEN, B. K., KALAMS, S. A., WALKER, B. D. & BALTIMORE, D. (1998). HIV-1 nef protein protects infected primary cells against killing by cytotoxic T lymphocytes. *Nature* **391,** 397–401.

DAAR, E. S., MOUDGIL, T., MEYER, R. D. & HO, D. D. (1991). Transient high levels of viremia in patients with primary human immunodeficiency virus type 1. *New Engl. J. Med.* **324,** 961–964.

D'ARGENIO, D. Z. & SCHUMITZKY. (1997). *ADAPT II User's Guide: Pharmacokinetic/Pharmacodynamics Systems Analysis Software.* Los Angeles: University of Southern California, Biomedical Simulations Resource.

DeBoer, R. J. & Perelson, A. S. (1998). Target cell limited and immune control models of HIV infection: a comparison. *J. theor. Biol.* **190,** 201–214.

Essunger, P. & Perelson, A. S. (1994). Modeling HIV infection of CD4+ T-cell subpopulations. *J. theor. Biol.* **170,** 367–391.

Guidotti, L. G., Rochford, R., Chung, J., Shapiro, M., Purcell, R. & Chisari, F. V. (1999). Viral clearance without destruction of infected cells during acute HBV infection. *Science* **284,** 825–829.

Haase, A. T. (1999). Population biology of HIV-1 infection: viral and CD4+ T cell demographics and dynamics in lymphatic tissues. *Ann. Rev. Immunol.* **17,** 625–656.

Ho, D. D., Neumann, A. U., Perelson, A. S., Chen, W., Leonard, J. M. & Markowitz, M. (1995). Rapid turnover of plasma virions and CD4 lymphocytes in HIV-1 infection. *Nature* **373,** 123–126.

Hraba, T., Dolezal, J. & Celikovsky, S. (1990). Model-based analysis of CD4+ lymphocyte dynamics in HIV infected individuals. *Immunobiology* **181,** 108–118.

Jin, X. Bauer, D. E., Tuttleton, S. E., Lewin, S., Gettie, A., Blanchard, J., Irwin, C. E., Safrit, J. T., Mittler, J., Weinberger, L., Kostrikis, L., Zhang, L., Perelson, A. S. & Ho, D. D. (1999). Dramatic rise in plasma viremia after CD8+ T-cell depletion in SIV-infected macaques. *J. Exp. Med.* **189,** 991–998.

Kahn, J. O. & Walker, B. D. (1998). Acute human immunodeficiency virus type 1 infection. *New Engl. J. Med.* **339,** 33–39.

Kaufmann, G. R., Cunningham, P., Kelleher, A. D., Zaunders, J., Carr, A., Vizzard, J., Law, M., Cooper, D. A. & the Sydney Primary HIV Infection Study Group. (1998). Patterns of viral dynamics during primary human immunodeficiency virus type 1 infection. *J. Infec. Dis.* **178,** 1812–1815.

Kirschner, D. E., Mehr, R. & Perelson, A. S. (1998). Role of the thymus in pediatric HIV-1 infection. *J. AIDS Human Retrovirol.* **18,** 95–109.

Klenerman, P., Phillips, R. E., Rinaldo, C. R., Wahl, L. M., Ogg, G., May, R. M., Mcmichael & Nowak, M. A. (1996). Cytotoxic T lymphocytes and viral turnover in HIV type 1 infection. *Proc. Nat. Acad. Sci. U.S.A.* **93,** 15323–15328.

Koup, R. A., Safrit, J. T., Cao, Y., Andrews, C. A., Mcleod, G., Borkowsky, W., Farthing, C. & Ho, D. D. (1994). Temporal association of cellular immune responses with the initial control of viremia in primary human immunodeficiency virus type 1 syndrome. *J. Virol.* **68,** 4650–4655.

Little, S. J., McLean, A. R., Spina, C. A., Richman, D. D. & Havlir, D. V. (1999) Viral dynamics of acute HIV-1 infection. *J. Exp. Med.* **190,** 141–150.

Maciaszek, J. W., Parada, N. A., Cruikshank, W. W., Center, D. M., Kornfeld, H. & Viglianti, G. A. (1997). IL-16 represses HIV-1 promoter activity. *J. Immunol.* **158,** 5–8.

Mackewicz, C. E., Blackbourn, D. J. & Levy, J. A. (1995). CD8+ T cells suppress human immunodeficiency virus replication by inhibiting viral transcription. *Proc. Nat. Acad. Sci. U.S.A.* **92,** 2308–231.

Matano, T., Shibata, R., Siemon, C., Connors, M., Lane, H. C. & Martin, M. A. (1998). Administration of an anti-CD8 monoclonal antibody interferes with the clearance of chimeric simian/human immunodeficiency virus during primary infections of rhesus macaques. *J. Virol.*, **72,** 164–169.

Mclean, A. R., Emery, V. C., Webster, A. & Griffiths, P. D. (1991). Population dynamics of HIV within an individual after treatment with zidovudine. *AIDS* **5,** 485–489.

Mclean, a. r. & kirkwood, T. B. L. (1990). A model of human immunodeficiency virus infection in T helper cell clones. *J. theor. Biol.* **147,** 177–203.

Mclean, A. R. & Nowak, M. A. (1992). Models of interactions between HIV and other pathogens. *J. theor. Biol.* **155,** 69–102.

Merrill, S. (1989). Modeling the interaction of HIV with cells of the immune response. In: *Mathematical and Statistical Approaches to AIDS Epidemiology* (C. Castillo-Chavez, ed.), Lecture Notes Biomathematics, Vol. 83, pp. 371–385. New York: Springer-Verlag.

Mittler, J. E., Markowitz, M., Ho, D. D. & Perelson, A. S. (1999). Improved estimates for HIV-1 clearance rate and intracellular delay. *AIDS* **13,** 1415–1417.

Murray, J. M., Kaufmann, G., Kelleher, A. D. & Cooper, D. A. (1998). A model of primary HIV-1 infection. *Math. Biosci.* **154,** 57–85.

Musey, L., Hughes, J., Schacker, T., Shea, T., Corey, L. & Mcelrath, M. J. (1998). Cytotoxic-T-cell responses, viral load, and disease progression in early human immunodeficiency virus type I infection. *New Engl. J. Med.* **337,** 1267–1274.

Nowak, M. A., May, R. M. & Anderson, R. M. (1990). The evolutionary dynamics of HIV-1 quasispecies and the development of immunodeficiency disease. *AIDS* **4,** 1095–1103.

Nowak, M. A., Anderson, R. M., Mclean A. R., Wolfs T. F., Goudsmit, J. & May, R. M. (1991). Antigenic diversity thresholds and the development of AIDS. *Science* **254,** 963–969.

Nowak, M. A. & Bangham, C. R. M. (1996). Population dynamics of immune responses to persistent viruses. *Science* **272,** 74–79.

Nowak, M. A., Lloyd, A. L., Vasquez, G. M., Wiltrout, T. A., Wahl, L. M., Bischofberger, N., Williams, J., Kinter, A., Fauci, A. S., Hirsch, V. M. & Lifson, J. D. (1997a). Viral dynamics in primary viremia and anti-retroviral therapy in simian immunodeficiency virus infection. *J. Virol.* **71,** 7518–7525.

Nowak, M. A., Bonhoeffer, S., Shaw, G. M. & May, R. M. (1997b). Anti-viral drug treatment: dynamics of resistance in free virus and infected cell populations. *J. theor. Biol.* **184,** 203–217.

Ogg, G. S., Jin, X., Bonhoeffer, S., Dunbar, P. R., Nowak, M. A., Monard, S., Segal, J. P., Cao, Y., Rowland-Jones, S. L., Cerundolo, V., Hurley, A., Markowitz, M., Nixon, D.F. & McMichael, A. J. (1998). Quantitation of HIV-1-specific cytotoxic T lymphocytes and plasma load of viral RNA. *Science* **279,** 2103–2106.

Pantaleo, G., Demarest, J. F., Schacker, T., Vaccarezza, M., Cohen, O. J., Daucher, M., Graziosi, C., Schnittman, S. S., Quinn, T. C., Shaw, G. M., Perrin, L., Tambussi, G., Lazzarin, A., Sekaly, R. P., Soudeyns, H., Corey, L. & Fauci, A. S. (1997). The qualitative nature of the primary immune response to HIV infection is a prognosticator of disease progression independent of the initial level of plasma viremia. *Proc. Nat. Acad. Sci. U.S.A.* **94,** 254–258.

PERELSON, A. S. (1989). Modeling the interaction of the immune system with HIV. In: *Mathematical and Statistical Approaches to AIDS Epidemiology* (C. Castillo-Chavez, ed.), Lecture Notes Biomathematics, Vol. 83, pp. 350–370. New York: Springer-Verlag.

PERELSON, A. S., KIRSCHNER, D. E. & DE BOER, R. (1993). Dynamics of HIV infection of CD4+ T cells. *Math. Biosci.* **114,** 81–125.

PERELSON, A. S. & NELSON, P. (1999). Mathematical analysis of HIV-1 dynamics *in vivo*. *SIAM Rev.* **41,** 3–44.

PERELSON, A. S., NEUMANN, A. U., MARKOWITZ, M., LEONARD, J. M. & HO, D. D. (1996). HIV-1 dynamics *in vivo*: virion clearance rate, infected cell life-span, and viral generation time. *Science* **271,** 1582–1586.

PHILLIPS, A. N. (1996). Reduction of HIV concentration during acute infection: independence from a specific immune response. *Science* **271,** 497–499.

RAMRATNAM, B., BONHOEFFER, S., BINLEY, J., HURLEY, A., ZHANG, L., MITTLER, J. E., MARKOWITZ, M., MOORE, J. M., PERELSON, A. S. & HO, D. D. (1999). Rapid production and clearance of HIV-1 and hepatitis C virus assessed by large volume plasma apheresis. *Lancet* **354,** 1782–1785.

REIBNEGGER, G., FUCHS, D., HAUSEN, A., WERNER, E. R., WENER-FELMAYER, G., DIERICH, M. P. & WACHTER, H. (1989). Stability analysis of simple models for immune cells interacting with normal pathogens and immune system retroviruses. *Proc. Nat. Acad. Sci. U.S.A.* **86,** 3026–2030.

RINALDO, C., HUANG, X., FAN, Z. F., DING, M., BELTZ, L., LOGAR, A., PANICALI, D., MAZZARA, G., LIEBMANN, J., COTTRILL, M. & GUPTA, P. (1995). High levels of anti-human immunodeficiency virus type 1 (HIV-1) memory cytotoxic T-lymphocyte activity and low viral load are associated with lack of disease in HIV-1-infected long-term nonprogressors. *J. Virol.* **69,** 5838–5842.

RIVIERE, Y., MCCHESNEY, M. B., PORROT, F., TANNEAU-SALVADORI, F., SANSONETTI, P., LOPEZ, O., PIALOUX, G., FEUILLIE, V., MOLLEREAU, M, CHAMARET, S., TEKAIA, F. & MONTAGNIER, L. (1995). Gag-specific cytotoxic responses to HIV type 1 are associated with a decreased risk of progression to AIDS-related complex or AIDS. *AIDS Res. Human Retroviruses* **11,** 903–907.

SACHSENBERG, N., PERELSON, A. S., SABINE, Y., SCHOCKMEL, G. A., LEDUC, D., HIRSCHEL, B. & PERRIN, L. (1998). Turnover of CD4 + and CD8+ T Lymphocytes in HIV-1 infection as measured by Ki-67 antigen. *J. Exp. Med.* **187,** 1295–1303.

SCHACKER, T., COLLIER, A., HUGHES, J., SHEA, T. & COREY, L. (1996). Clinical and epidemiologic features of primary HIV infection. *Ann. Int. Med.* **125,** 257–264.

SCHENZLE, D. (1994). A model for AIDS pathogenesis. *Statist. Med.* **13,** 2067–2079.

SCHMITZ, J. E., KURODA, M. J., SANTRA, S., SASSEVILLE, V. G., SIMON, M. A., LIFTON, M. A., RACZ, P., TENNER-RACZ, K., DALESANDRO, M., SCALLON, B. J., GHRAYEB, J., FORMAN, M. A., MONTEFIORI, D. C., RIEBER, E. P., LETVIN, N. L. & REIMANN, K. A. (1999). Control of viremia in simian immunodeficiency virus infection by CD8 + lymphocytes. *Science* **283,** 857–1586–860.

SCHNITTMAN, S. M., LANE, H. C., GREENHOUSE, J., JUSTEMENT, J. S., BASERLER, M. & FAUCI, A. S. (1990). Preferential infection of CD4 + memory T cells by human immunodeficiency virus type-1: evidence for a role in the selective T-cell functional defects observed in infected individuals. *Proc. Nat. Acad. Sci. U.S.A.* **87,** 6058–6052.

STEVENSON, M., STANWICK, T. L., DEMPSEY, M. P. & LAMONICA, C. A. (1990). HIV-1 replication is controlled at the level of T cell activation and proviral integration. *EMBO J.* **9,** 1551–1560.

STILIANAKIS, N. I., DIETZ, K. & SCHENZLE, D. (1997). Analysis of a model for the pathogenesis of AIDS. *Math. Biosci.* **145,** 27–46.

WALKER, C. M., MOODY, D. J., STITES, D. P. & LEVY, J. A. (1986). CD8+ lymphocytes can control HIV infection in vitro by suppressing virus replication. *Science* **234,** 1563–1566.

WEI, X., GHOSH, S. K., TAYLOR, M. E., JOHNSON, V. A., EMINI, E. A., DEUTSCH, P., LIFSON J. D., BONHOEFFER, S., NOWAK, M. A., HAHN, B. H., SAAG, M. S. & SHAW, G. (1995). Viral dynamics in human immunodeficiency virus type 1 infection. *Nature* **373,** 117–123.

WU, H., KURITZKES, D. R., MCCLERNON, D. R., KESSLER, H., CONNICK, E., LANDAY, A., SPEAR, G., HEATH-CHLOZZI, M., ROUSSEAU, F., FOX, L., SPRITZLER, J., LEONARD, J. M. & LEDERMAN, M. M. (1999). Characterization of viral dynamics in human immunodeficiency virus type-1 infected patients treated with combination antiretroviral therapy; relationships to host factors, cellular restoration, and virologic end points. *J. Infect. Dis.* **179,** 799–807.

ZACK, J., HAISLIP, A., KROGSTAD, P. & CHEN, I. (1992). Incompletely reverse-transcribed human immunodeficiency virus type 1 genomes in quiescent cells can function as intermediates in the retroviral life cycle. *J. Virol.* **66,** 1717–1725.

ZHANG, Z.-Q., SCHULER, T., ZUPANCIC, M., WIETGREFE, S., STASKUS, K. A., REIMANN, K. A., REINHART, T. A., ROGAN, M., CAVERT, W., MILLER, C. J., VEAZEY, R. S., NOTERMANS, D., LITTLE, S., DANNER, S. A., RICHMAN, D. D., HAVLIR, D., WONG, J., JORDAN, H. L., SCHACKER, T. W., RACZ, P., TENNER-RACZ, K., LETVIN, N. L., WOLINSKY, S. & HAASE, A. T. (1999). Sexual transmission and propagation of SIV and HIV in resting and activated $CD4^+$ T cells. *Science* **286,** 1353–1357.

APPENDIX A

In Section 2.2 it was asserted that two pairs of parameters (T_0 and π, c and π) in the simplified model are dependent. We now make that statement precise.

A.1. DEPENDENCY OF T_0 AND π

Suppose the uninfected equilibrium requirement, $\lambda = dT_0$ is used to eliminate the source term, λ, in eqn (1), and define the initial-value problem IVP1 by

$$\frac{dT(t)}{dt} = d(T_0 - T) - kTV, \quad T(0) = T_0$$

$$\frac{dT^*(t)}{dt} = kTV - \delta T^*, \quad T^*(0) = T_0^*, \quad \text{(IVP1)}$$

$$\frac{dV(t)}{dt} = \pi T^* - cV, \quad V(0) = V_0$$

Let $\phi(t) = [\phi_1(t)\ \phi_2(t)\ \phi_3(t)]^T$ be the unique solution on some interval of interest, $[0, t_f]$. Define a second initial value problem, IVP2, by

$$\frac{d\tilde{T}(t)}{dt} = d(\tilde{T}_0 - \tilde{T}) - k\tilde{T}V, \quad \tilde{T}(0) = \tilde{T}_0,$$
$$\frac{d\tilde{T}^*(t)}{dt} = k\tilde{T}V - \delta\tilde{T}^*, \quad \tilde{T}^*(0) = \tilde{T}^*_0, \quad \text{(IVP2)}$$

$$\frac{dV(t)}{dt} = \tilde{\pi}\tilde{T}^* - cV, \quad V(0) = V_0.$$

If $\tilde{T}_0 = \sigma T_0$ and $\tilde{\pi} = (1/\sigma)\pi$, then IVP2 has solution $\tilde{\phi}(t) = [\sigma\phi_1(t)\ \sigma\phi_2(t)\ \phi_3(t)]^T$ on the interval $[0, t_f]$.The proof is immediate.

The consequence of this result is that either the nominal target cell density, T_0, or the virion production constant, π, can be sought in parameter estimation using measurements of viral load alone, but not both. If methods are devised to make independent measurements of either of these, then the other can be sought using parameter estimation schemes such as the one we use in Section 2 which uses only viral load data.

A.2. DEPENDENCY OF c AND π

When $c \gg \delta$, a quasi-steady state approximation is sometimes used (Nowak *et al.*, 1997b) to reduce the system of three equations in the simplified model to two differential equations and one algebraic equation:

$$\frac{dT(t)}{dt} = d(T_0 - T) - \frac{k\pi}{c} TT^*,$$

$$\frac{dT^*(t)}{dt} = \frac{k\pi}{c} TT^* - \delta T^*,$$

$$\bar{V} \equiv \frac{\pi}{c} T^*.$$

Numerically it has been verified that, for the values of c and δ in Table 2, this system of equations gives solutions that are nearly identical with the original system. We note that neither π nor c appears individually but always as a ratio. Hence, we cannot distinguish between these two quantities from viral load data alone.